

# A CAD system for cerebral glioma in Magnetic Resonance Diffusion Tensor Images: semiautomatic segmentation and therapy follow up

Giorgio De Nunzio<sup>a</sup>, Marina Donativi<sup>a</sup>, Gabriella Pastore<sup>b</sup>, Antonella Castellano<sup>c</sup>,  
Andrea Falini<sup>c</sup>, Lorenzo Bello<sup>d</sup>, Riccardo Soffietti<sup>c</sup>

<sup>(a)</sup>Dipartimento di Scienza dei Materiali–Università del Salento, Via Provinciale Lecce-Monteroni, 73100 Lecce, Italy

<sup>(b)</sup>U.O.C. Fisica Sanitaria-Ospedale V. Fazzi, Piazza Muratore, 73100 Lecce, Italy

<sup>(c)</sup>Unità di Neuroradiologia CERMAC–Ist. Sc. e Univ Vita-Salute San Raffaele –Via Olgettina,60, 20132 Milano, Italy

<sup>(d)</sup>Unità di Neurochirurgia – Dip. di Scienze Neurologiche – Univ.di Milano, Via Sforza 35, 20122 - Milano, Italy

<sup>(d)</sup>Neuro-oncologia – Dip. di Neuroscienze e Oncologia – Università di Torino, Via Cherasco 15, 10126 Torino, Italy

Tel: +39 (0) 832297084, Fax: +39 (0) 832 297100, e-mail: giorgio.denunzio@unisalento.it

## Abstract

Tumor cells in cerebral glioma invade surrounding tissues preferentially along white matter tracts, spreading beyond the abnormal area seen on conventional Magnetic Resonance Images (MRI). Diffusion tensor imaging (DTI) can reveal larger peritumoral abnormalities in gliomas that are not apparent on MRI.

Our aim was the characterization of pathological vs healthy tissue in DTI datasets by 3D statistical texture analysis, developing a semi automatic segmentation technique (CAD, Computer Assisted Detection system) for cerebral glioma, especially useful in patient follow-up during chemotherapy and for preoperative assessment of tumor extension.

## INTRODUCTION

Cerebral gliomas are the most common primary brain tumors. They are characterized by diffuse and infiltrative growth, which is the major determinant of their poor prognosis; therefore, an early diagnosis and a comprehensive evaluation of tumor extent and relationship with surrounding anatomical structures are decisive in determining prognosis and treatment planning. Tumor cells invade surrounding tissues preferentially along white matter (WM) tracts, spreading beyond the abnormal area seen on conventional magnetic resonance (MR) images [1]. Therefore conventional MR does not always permit a precise delineation of tumor margins or tumor differentiation from oedema or treatment effects.

On the contrary, Diffusion Tensor Imaging (DTI) is sensitive to subtle disruption of WM tracts and can detect abnormalities around gliomas in regions that

appear normal on conventional imaging. DTI is a technique sensitive to the ordered anisotropic diffusion of water along WM tracts, and can detect the presence of tumor cell infiltration in WM around the edge of the gross tumor [2,3].

By extracting and quantifying the information from the diffusion tensor, various metrics can be calculated. These scalar or vector entities can identify different physiological and pathological characteristics in the same tissue. Recently, an approach has been proposed [4], which is based on the mathematical decomposition of the diffusion tensor into its isotropic ( $p$ ) and anisotropic ( $q$ ) components; this approach allows to determine tissue diffusion 'signatures', that demonstrate different aspects of tumour behaviour, at the level of both tumor core and peritumoral WM.

By splitting the diffusion tensor into its isotropic and anisotropic components, it is possible to define two regions around a tumour: an internal one (the core of the tumour, hereafter called "Q area") characterized by reduced anisotropy and, around this area, a region of increased isotropic but normal anisotropic diffusion ("P area") which correlates with glioma infiltration, as described in previous studies and confirmed by image-guided biopsies. The P area is generally larger than the Q area. Figure 1 shows a T2-weighted image where the region of interest (ROI) drawn from a  $q$  map (cyan) and from the corresponding  $p$  map (yellow) are overlapped:  $p$  abnormalities are larger than  $q$  abnormalities.

On the basis of the richness of information of these images, we decided to develop a Computer-Assisted Detection (CAD) system for the recognition of cerebral gliomas in DT images.

The resulting system can identify tumor regions in

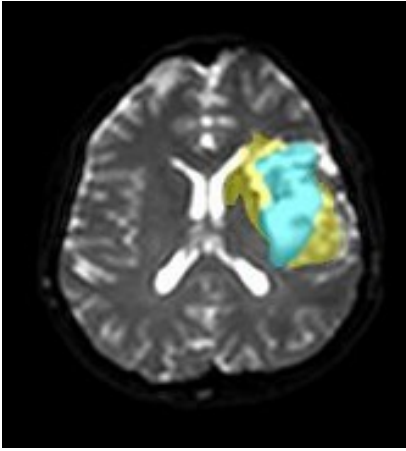


**Figure 1:** Morphological image on which tumoral ROIs drawn on the  $p$  map (yellow, larger, “P area”) and on  $q$  map (cyan, smaller “Q area”) are overlapped.

brain tissue, either automatically or semi-automatically, i.e. starting from a mouse click on an image location chosen by the physician as belonging to pathological tissue. It allows objective tumor identification and quantitative measurements, such as glioma extension, especially in view of a patient follow-up during therapy planning.

The system is also the support for an alternative method for therapy follow-up based on the variation of brownian motion of water within tumor tissue as an indicator of the success of chemotherapy and tumor involution. In fact, after a successful treatment, we expect to observe changes in tumor water diffusion due to cell kill effects. Furthermore, the subsequent restructuring of the heterogeneous tumor fibers due to the changes in cell density and to the decrease in volume of extracellular water content, may lead to heterogeneous changes in the underlying tissue morphology. The result is a change of anisotropy and isotropy values (e.g.  $q$  or  $p$ ) [2,4] in tumor regions (in particular, we expect a decrease of  $p$  and an increase of  $q$  values). [1,3]

## MATERIALS AND METHODS

### Materials

We selected fifteen patients with glioma (9 low-grade, 6 high-grade) a 6 healthy control patients. 3T MR-DTI consisted of a single-shot EPI sequence with 32 diffusion gradient directions at a b-value of 1000  $\text{s}/\text{mm}^2$  and one image set without diffusion weighting. The sequence was repeated two consecutive times and data were averaged off-line to increase sig-

nal-to-noise ratio.

T2-weighted FSE and T1-weighted FFE conventional imaging was performed for anatomic guidance and morphological characterization of the lesions.

DTI datasets were aligned off-line to the echo-planar volume without diffusion weighting on a PC workstation using the AIR software to correct artifacts due to rigid body movement during scan acquisition.

### Methods: the CAD system

The developed system adheres to the typical scheme of a CAD software tool, with (a) data preprocessing, (b) feature calculation and (c) supervised tissue classification by an Artificial Neural Network (ANN) (Figure 2). The development process is summed up hereunder:

- Diffusion maps were calculated from DT images using an in-house software implemented in Matlab, producing fractional anisotropy (FA) and mean diffusivity (MD or  $\langle D \rangle$ ) maps, and  $p$  and  $q$  maps (the isotropic and anisotropic components of the diffusion tensor).

Manual segmentation of pathological areas was performed on each map by two neuroradiologists:

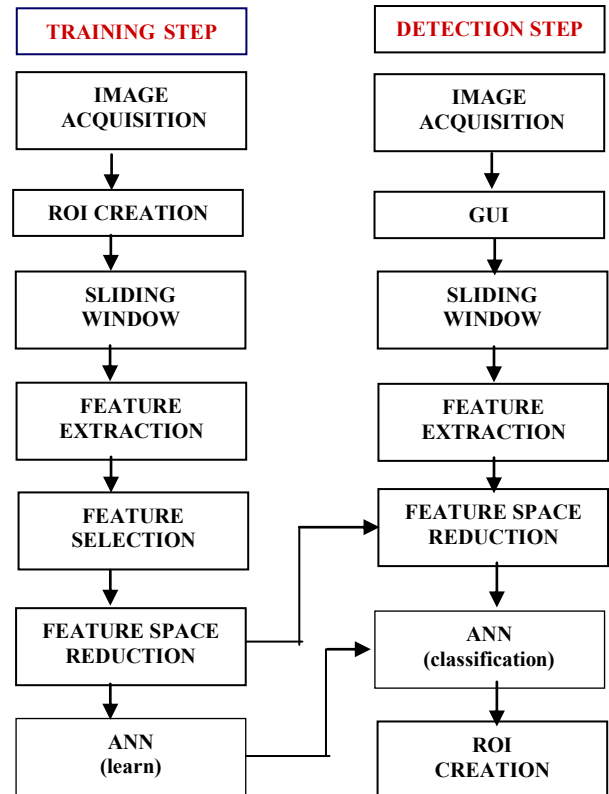


**Figure 2 :** Flowchart of the CAD system, training (left) and detection (right) steps

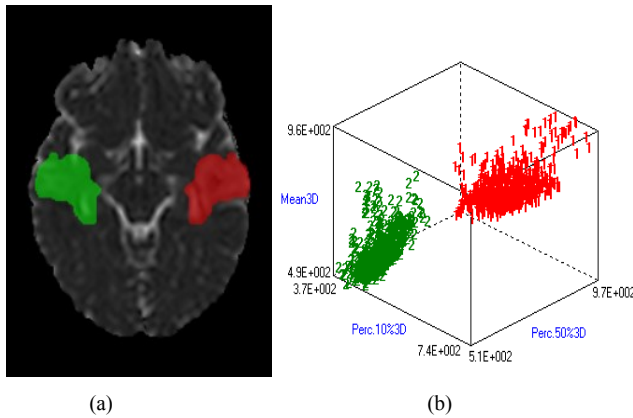


**Figure 3.** a) The tumor (red region, manually drawn) and the healthy ROI (contralateral, green region) on a slice of the  $p$  map of a patient. b) Scatter plot of three of the best features, for the  $p$  map. Red 1's are pathological svois, while green 2's represent the corresponding contralateral healthy regions.

ROIs in the different maps were drawn independently from one another, in different moments, so that the physicians were not conditioned by already performed segmentations.

Each ROI drawn by the physicians was explored with a sliding window technique, in order to train the supervised classifier to learn typical patterns of healthy and pathological tissue regions.

At each sliding step, the window covers an image sub-volume (*svoi*). Each *svoi* is retained for classifier training if the *svoi* central voxel is pathological. At the same time, a contralateral sub-box (called *csvoi*) is considered if it has a healthy central voxel. This procedure gave us some thousand couples of small pathological and healthy *svois/csvois* (per patient and per map), respectively extracted from the original tumor ROI and from the contralateral region.

b) From these sub-vois, statistical feature calculation from the intensity and the gradient histogram, from the cooccurrence matrix (COM) and the run length matrix (RLM) was carried out [5] and scatter plots were drawn after choosing the most discriminant ('best') features according to the Fisher-filter score (Figure 3). The ten best features were chosen for each map and patient; then a global set  $F$  composed of about ten features was built, by choosing the best features common to all the patients.

To eliminate redundancy of information, we reduced the feature-space dimensionality by using principal component analysis (PCA). We decided to retain the minimum set of principal components

that explained at least 97% of the variance.

c) We used a feed-forward ANN with back-propagation, implemented in Matlab using *PRTools*, a system for pattern recognition based on the *Neural Network Toolbox*. The network architecture consisted of a hidden layer with three neurons and one output neuron.

The network was applied to the test data set and its performance assessed by the receiver operating characteristic (ROC) curve (sensitivity vs 1-specificity, at different values of the ANN decision threshold).

To help the physician in the assisted diagnosis and to optimize interactivity by the radiologist, a Matlab GUI (Graphical User Interface) was created: it starts from image loading, goes through the extraction of a rough bounding box containing the tumor lesion, calculates the texture features (again by a sliding window) and computes by the trained ANN the probability of presence of tumor tissue in each brain sub-volume. Once probability maps are calculated, by choosing a suitable threshold on probability it is possible to select tissues that are above it, and segment the image into probably healthy and probably tumoral regions. By thresholding, a segmented image can now be produced.

#### **Methods: application of CAD system in therapy follow up**

Starting from the analysis of the diffusion tensor and by using a Matlab script, maps of  $p$  isotropy for five patients before and after five cycles of chemotherapy were carried out. In the medical protocol, patients with suspected low grade glioma, who are unresectable or candidate to a partial resection only, and have undergone a diagnostic biopsy, and patients who had a partial resection at first surgery and have progressed clinically (increasing seizures) and/or radiologically were included.

After a step of realignment of the DTI maps before and after the chemotherapy (using an in-house software implemented in Matlab) isotropy  $p$  maps before chemotherapy were analyzed by the CAD tool, which returned the ROIs of tumor tissue. Each ROI was then overlapped to the isotropy maps after treatment. A comparison between the tumor tissue located by the ROIs (before and after treatment) was carried out with a voxel-by-voxel approach: for each patient,  $p$  values of each voxel within the tumor ROI after therapy ( $p_2$ ) were plotted as a function of their pre-therapy values ( $p_1$ ). All tumor voxels were classified into three classes: red-labeled voxels for which the  $p$

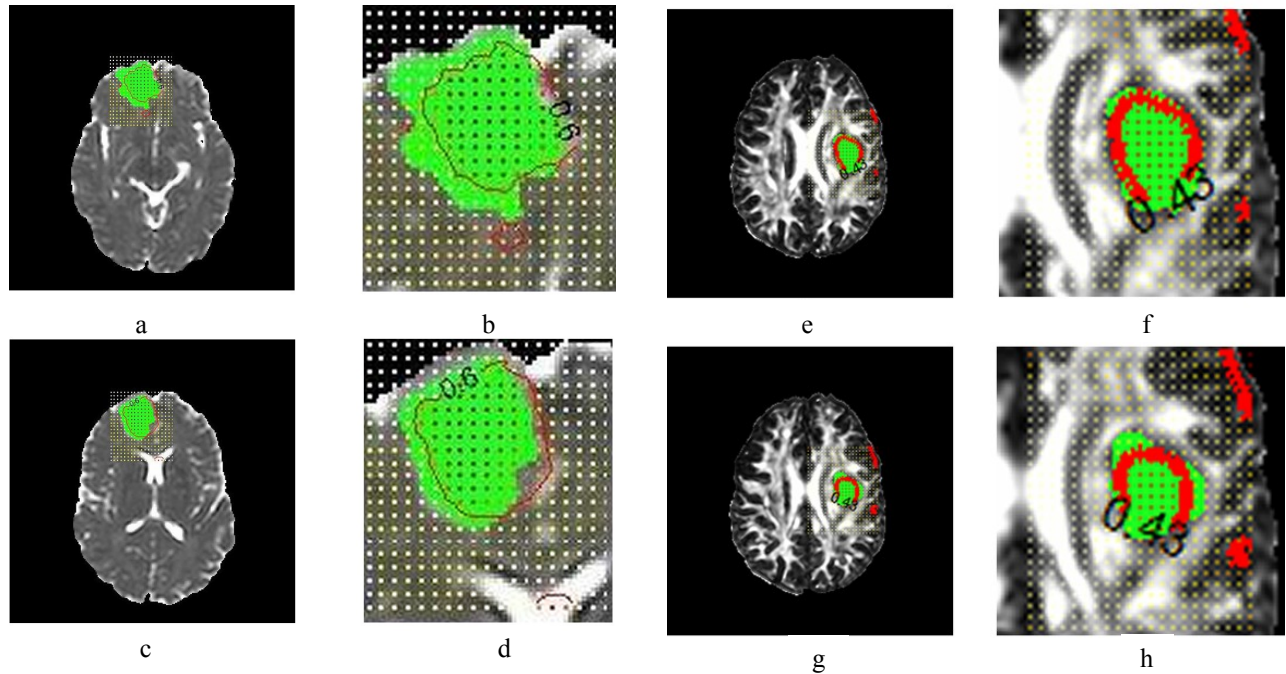


**Figure 4.** The CAD probability map is displayed by a parallelepiped grid of color dots, where cold colors correspond to lower probability of tumor, and warm colors to higher malignancy likelihood. Each dot is the center of the sliding window. The red line is the result of CAD segmentation. The green region is the physician’s ROI. (a, c)  $p$  and (e, g)  $q$  maps of a pathological patient; (b, d, f, h) a detail of the maps.

value considerably increased (with respect to a suitable threshold  $\theta$ :  $\Delta p = p_2 - p_1 > \theta$ ), blue-labeled voxels for which the  $p$  values decreased significantly ( $\Delta p < -\theta$ ), and green-labeled voxels for which the  $p$  values did not change appreciably ( $|\Delta p| < \theta$ ) [6-8]. The two significant color  $p$  values (red and blue ones) was overlaid on the  $p$  map before treatment.

## RESULTS AND DISCUSSION

Preliminary results were obtained for the  $p$  map (AUC = 0.96) and the FA map (AUC = 0.98). Test images were automatically segmented by tissue classification and thresholding. In order to qualitatively assess segmentation performance, we visually compared probability maps and automatic segmentations with the corresponding manual segmentations.

In Figure 4, the dots mark the positions of the sliding window (svoici centers). Each of these points is assigned a color from a color scale: cold colors for low probability values of tumor, warm colors for high values. The red line shows the segmentation produced by the CAD system with the ANN output threshold that is the optimal value at which sensitivity equals specificity. The green region is the corresponding manually drawn ROI. The computed segmentations are in acceptable accord with the tumor contours as drawn by the radiologist.

In Figure 5 and 6 some results about therapy follow up are presented: a successful case and an unsuccessful one are shown. In particular, Figure 5a displays the distribution of the  $p$  changes for the entire tumor volume, while Figures 5b and 5c show the regions of significant variation on the  $p$  map. It is possible to note the large areas of  $p$  decrease (the blue areas in Figures 5b and 5c); they indicate regions where the isotropic diffusivity of water decreased, probably due to reorganization of the white fibers. Furthermore, these areas were electrically stimulated during the post-chemo surgery and they presented conduction times very short due to the presence of highly compact fibers.

In figure 6, a negative response to chemotherapy is presented. In the red parts of Figure 6b and 6c, the tumor grew into the brain tissue, thus the infiltration (and  $p$  values) increased. Moreover, the RGB graph (Figure 6a) shows more red pixels than blue ones; this is a further evidence of the increased infiltration (and according to this study, there was no response to chemotherapy).

## CONCLUSIONS

This paper describes a method for automatic detection of cerebral glioma in brain DT-MR scans, by means of a neural classifier trained on statistical tex-

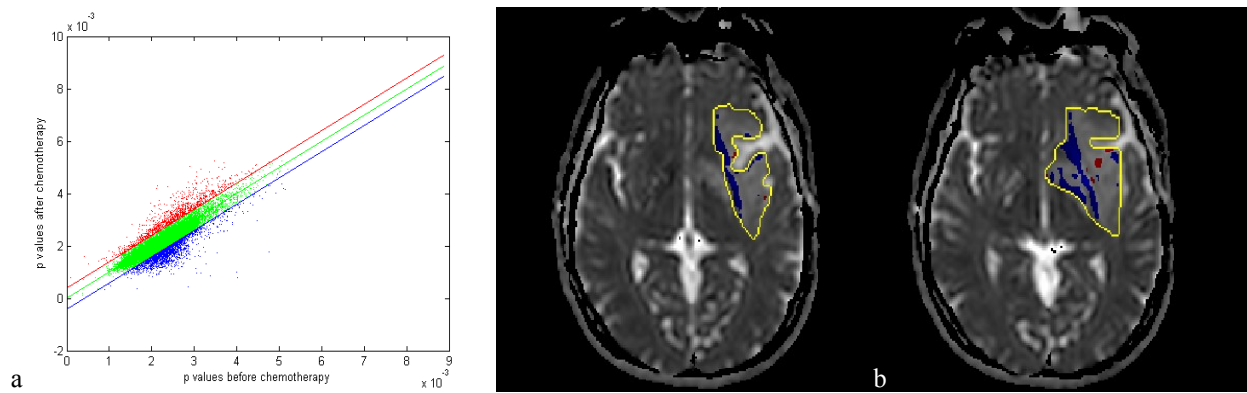


**Figure 5** A successful case of therapy. a) Distribution of p changes for the entire tumor volume. The red, green and blue pixels indicate regions of increased, unchanged and decreased isotropy diffusion, respectively. b) A region of p decrease inside the tumor (blue area): these areas were electrically stimulated during the post chemo surgery and presented conduction times very short due of the presence of highly compact fibers.

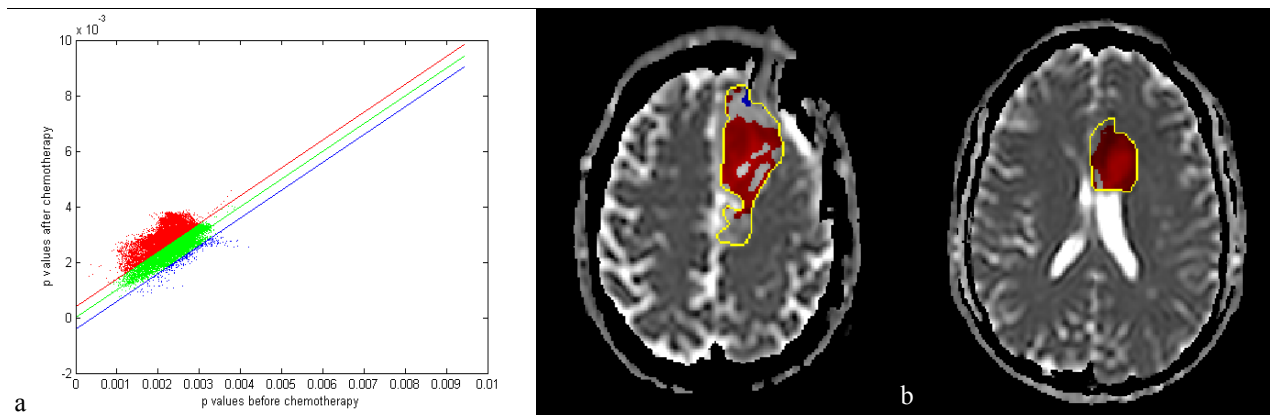


**Figure 6** a) The RGB graph for a negative response to chemotherapy. The red pixels are more than the blue ones. b) Two regions of p increase due to an increased tumor infiltration.

ture features. The use of textural features in diffusion images, with the aim of identifying brain tumor regions, is, at the best of our knowledge, a new approach.

In order to build a CAD system, we characterized healthy and pathologic tissue by the use of statistical textural features, calculated by a sliding window method. We proved that the selected features discriminated very well the healthy regions from the tumor ones in p and FA maps.

We then investigated and demonstrated the potential of Artificial Neural Networks as the supervised classifier system: a ANN (back-propagation, feed-forward, 1-hidden-layer network) was trained and applied to a test set, performing very well, with high scores as measured by the ROC area under the curve. The trained ANN allowed tissue classification and the computation of malignancy-probability maps, giving the probability of each small brain subvolume (svoi) to be tumor tissue.

After threshold application, the computed segmentations are in acceptable accord with the tumor contours as drawn by the radiologist.

## REFERENCES

- [1] S.J.Price, R.Jena, N.G.Burnet, T.A.Carpenter, J.D.Pickard, J.H.Gillard, Predicting patterns of glioma recurrence using diffusion tensor imaging, *Eur Radiol*, 2007;17(7):1675-84.
- [2] S. J. Price et al., Tissue signature characterisation of diffusion tensor abnormalities in cerebral gliomas. *Eur Radiol* 2004;14(10):1909-17.
- [3] S. J. Price et al., Improved delineation of glioma margins and regions of infiltration with the use of diffusion tensor imaging: An image guided biopsy study, *AJNR Am J Neuroradiol*, 2006;27(9):1969-74.
- [4] A.Pena, H.A.Green, T.A.Carpenter, S.J.Price, J.D.Pickard, J.H.Gillard, Enhanced visualization and quantification of magnetic resonance diffusion tensor

- imaging using the p:q tensor decomposition., *Br J Radiol* 2006;79(938):101-9.
- [5] R. Haralick, K. Shanmugam, I. Dinstein, Textural features for image classification. *IEEE Trans Syst Man Cybern* 1973. 6:610-21
- [6] B.A.Moffat et al., Functional diffusion map: A noninvasive MRI biomarker for early stratification of clinical brain tumor response, *PNAS*, 2005;102(15): 5524–5529
- [7] D.A.Hamstra et al., Functional Diffusion Map As an Early Imaging Biomarker for High-Grade Glioma: Correlation With Conventional Radiologic Response and Overall Survival, *JCO*, 2008: 28(20): 3387-3394.
- [8] C.J.Galban et al., A Feasibility Study of Parametric Response Map Analysis of Diffusion-Weighted Magnetic Resonance Imaging Scans of Head and Neck Cancer Patients for Providing Early Detection of Therapeutic Efficacy, *TransOnc*, 2009; 2(3): 184-190.